Available online at www.sciencedirect.com
ScienceDirect
Journal of Power Sources 168 (2007) 434–446
JOURNAL OF POWER SOURCES
www.elsevier.com/locate/jpowsour

Water and air management systems for a passive direct methanol fuel cell

Gregory Jewett, Zhen Guo, Amir Faghri *

Department of Mechanical Engineering, University of Connecticut, Storrs, CT 06269, USA

Received 9 February 2007; received in revised form 15 March 2007; accepted 16 March 2007
Available online 30 March 2007

Abstract

In this paper water and air management systems were developed for a miniature, passive direct methanol fuel cell (DMFC). The membrane thickness, water management system, air management system and gas diffusion electrodes (GDE) were examined to find their effects on the water balance coefficient, fuel utilization efficiency, energy efficiency and power density. Two membranes were used, Nafion® 112 and Nafion® 117. Nafion® 117 cells had greater water balance coefficients, higher fuel utilization efficiency and greater energy efficiency. A passive water management system which utilizes additional cathode gas diffusion layers (GDL) and a passive air management system which makes use of air filters was developed and tested. Water management was improved with the addition of two additional cathode GDLs. The water balance coefficients were increased from −1.930 to 1.021 for a cell using a 3.0 mol kg^{-1} solution at a current density of 33 mA cm^{-2}. The addition of an air filter further increased the water balance coefficient to 1.131. Maximum power density was improved from 20 mW cm^{-2} to 25 mW cm^{-2} for 3.0 mol kg^{-1} solutions by upgrading from second to third generation GDEs, obtained from E-TEK. There was no significant difference in water management found between second and third generation GDEs. A fuel utilization efficiency of 63% and energy efficiency of 16% was achieved for a 3.0 mol kg^{-1} solution with a current density of 66 mA cm^{-2} for third generation GDEs.

Keywords: Direct methanol fuel cell; Water management; Air breathing; Passive

1. Introduction

A growing demand in portable electronic power supplies has forced the market to look for new technology to power devices. Direct methanol fuel cells (DMFC) have the potential to have greater power density, longer runtime, instant recharging and lower weight than conventional batteries [1–5]. The most significant obstacle for DMFC development is methanol crossover, a process where methanol will diffuse through the membrane generating heat but no power [6]. This problem can be limited if the concentration of methanol at the anode can be maintained between 2.0 mol kg^{-1} and 3.0 mol kg^{-1}. However, this significantly reduces the energy density of the system since water will produce no power and will take up a large volume in the fuel reservoir. Storing pure methanol is the most efficient method of fuel storage and water can be supplied from either an external source or recovered from the reactions. This paper is focused on the recovery of water from the reactions to supply the anode with water, so that water neutral operation can be achieved.

A DMFC is an electrochemical device that converts chemical energy stored in methanol into electrical energy [7]. The reactions that take place in a DMFC are given below:

$$\text{Anode}: \ CH_3OH + H_2O \rightarrow CO_2 + 6H^+ + 6e^- \quad (1)$$

$$\text{Cathode}: \ 6H^+ + 6e^- + 1.5O_2 \rightarrow 3H_2O \quad (2)$$

$$\text{Overall}: \ CH_3OH + 1.5O_2 \rightarrow CO_2 + 2H_2O \quad (3)$$

The anode reaction requires that a molecule of water is used for every molecule of methanol consumed, and the products of this reaction are carbon dioxide and hydrogen ions. At the cathode, oxygen is reduced with hydrogen ions to create three molecules of water. A net output of two water molecules and one carbon dioxide molecule is produced in the overall reaction. There is also heat created due to the irreversibility of this reaction and methanol crossover. Water is also transported through the membrane through methods other than the reaction.

* Corresponding author. Tel.: +1 860 486 0419; fax: +1 860 486 5088.
E-mail address: faghri@engr.uconn.edu (A. Faghri).

0378-7753/$ – see front matter © 2007 Elsevier B.V. All rights reserved.
doi:10.1016/j.jpowsour.2007.03.052

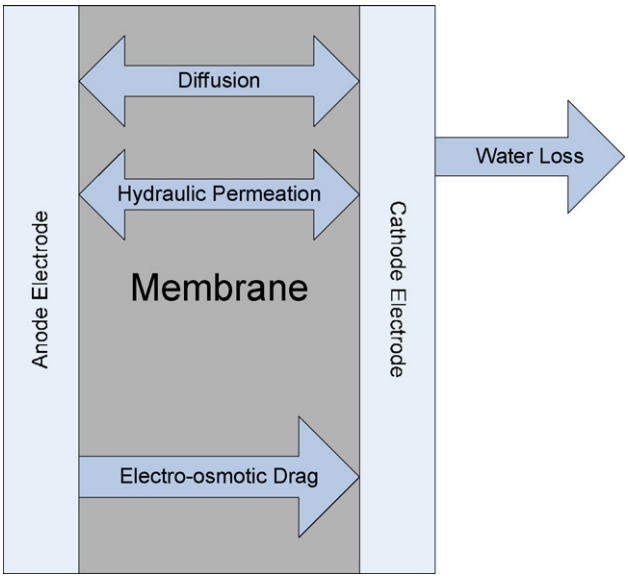

Fig. 1. Water transport mechanisms in DMFC membrane.

Water transport in the membrane takes place by diffusion, hydraulic permeation and electro-osmotic drag, as shown in Fig. 1. Diffusion of water takes place due to species and concentration gradients. Hydraulic permeation is caused by pressure gradients across the membrane. Electro-osmotic drag (EOD) in the cell is caused by hydrogen protons pulling water through the membrane. Liu et al. [8] states that for a thick membrane, such as Nafion® 117, 15 water molecules are dragged through the membrane for every proton and three molecules are created from the reaction. At higher current densities this becomes the primary form of water transport.

Ren et al. [9] studied EOD by limiting diffusion and hydraulic permeation with sufficiently high current density and equal anode and cathode pressures. Using an MEA with an active area of 5 cm^2 and high 1.0 M methanol and O_2 flow rates the water transport was found to be insensitive to methanol solution flow rate. They determined that electro-osmotic drag was independent of current density up to 600 mA cm^{-2} and increased significantly with temperature. Ratios of 2.0 molecules of water to hydrogen protons were recorded at 15 °C and increased to 5.1 molecules of water to hydrogen protons at 130 °C.

Further studies conducted by Ren and Gottesfeld [10] found other factors that influence the electro-osmotic drag of water in perfluorosulfonic acid (PFSA) membranes, i.e. Nafion®. The factors that influence electro-osmotic drag are temperature, membrane water content and membrane equivalent weight. Comparing a dried membrane to a fully hydrated membrane at different temperatures it was found that at low temperatures the dried membrane maintains a lower but stable water content, resulting in a lower but stable drag coefficient. For Nafion® membranes it was found that higher equivalent weight membranes have a lower electro-osmotic drag coefficient.

Understanding the three mechanisms of water transport allows for many methods of supplying water to the anode, which consist of active and passive approaches. Active methods consist of water traps and pumps to clear the cathode of water and recirculate it to the anode. Zhang et al. [11] studied active methods of removing water from the cathode of a polymer electrolyte fuel cell by droplet detachment through high air velocity shear force. Passive methods have no moving parts and the benefit is that they have simpler designs and lower weight. These methods rely on hydraulic permeation of water, some of which are described below.

Peled et al. [12] developed a hydrophobic liquid-water leakproof layer which was applied to both sides of the cathode current collector. This layer was a paste that consisted of 20–50% Teflon and carbon powders. The paste was applied to give a thickness of 20–50 μm which restricted the leaking of water. This creates a hydraulic pressure at the cathode which forces water to move back to the anode side of the cell. Using this liquid-water leakproof layer, Blum et al. [13] managed to decrease W (the water molecules lost per molecule of methanol consumed) from 7 to 2, which represents only the production of water from the reaction was being lost; water neutral operation. It was even possible to decrease W to 0.5 meaning that excess water needed to be removed from the cell.

Lu et al. [14] designed a membrane electrode assembly (MEA) that utilizes a microporous layer (MPL) to increase the hydraulic pressure on the cathode side of the cell. The MPL is a 30 μm thick carbon paper with a coating of Vulcan XC72R carbon black and 40 wt% Teflon. Lu et al. [14] defined a water transport coefficient as $\alpha = j_m F/I$, where j_m is the water flux to the cathode, I the current density and F is the Faraday constant. The MPL reduced α to 0.05 at room temperature, 0.16 at 40 °C and 0.64 at 60 °C compared to electro-osmotic drag coefficients of 2.08 at 23 °C, 2.5 at 40 °C and 3.0 at 60 °C. This is a significant decrease in water loss due to electro-osmotic drag, 2.34 at 40 °C and 2.36 at 60 °C. Kim et al. [15] also designed a novel MEA which increased the water back diffusion as well as the performance. Power density of about 50 mW cm^{-2} were reported for the novel MEA structure, an increase of about 8 mW cm^{-2} over the conventional design. Water back diffusion efficiency was also increased from 12% to 21% using Nafion® 112 membranes in the conventional and novel MEAs.

In this study, a passive approach for water and air management in the DMFC will be explored. The water management system will consist of additional thick, hydrophobic gas diffusion layers at the cathode of the cell. This layer should create a hydraulic pressure at the cathode of the cell which will drive water created from the reaction back across the membrane to the anode.

To further increase cell performance, reduce water evaporation and protect the cell an air management system is needed. The air management system consists of an air filter which can block small airborne particles, increase the cell temperature via thermal insulation and reduce the rate of water loss due to evaporation. The air filter needs to be easily replaceable to allow for new clean filters to be added to the cell. By reducing the amount of water lost from the cell the water management system can recirculate more water to the anode of the cell, thus keeping the methanol concentration stable. It will also provide a waterproofing layer that will protect the cathode from external water flooding the cathode. This is especially important for

applications where the cell is exposed to environmental conditions such as rain. In addition the air management system will provide thermal insulation so that the temperature of the cell will be increased, thus providing better performance and power.

The air management system will consist of a filter external to the cell which will provide filtration, thermal insulation and reduce the evaporation of water from the cathode of the cell. The effects of methanol concentration as well as electrical loading will be examined for each cell. The electrical performance as well as the temperature, water and methanol transport will be examined for these tests.

2. Experimental procedure

This section will discuss the design, assembly and testing procedures that were used. The cells used in this study are miniature passive DMFCs, with an active area of 9 cm^{-2}. Parameters that were changed were the water management system, air management system, gas diffusion electrodes (GDE) and membrane thickness. The water balance coefficient, power density, fuel utilization efficiency and energy efficiency were examined.

The structure and MEA of the cell is the same as described in Guo and Faghri [16]. The membranes used were Nafion® 112 and Nafion® 117 which were hot pressed together with the anode and cathode gas diffusion layers. Platinum coated niobium expanded metal mesh is used as the current collector on both sides of the membrane electrode assembly (MEA). The layers are held together using a fiberglass window frame structure with ribs. A reservoir is attached to the anode side of the cell and is sealed using a rubber gasket next to the frame.

This research group has used three different GDEs for the anode and cathode. A GDE consists of a gas diffusion layer (GDL) with a specified catalyst loading. A first generation GDE was made in house as described in Guo and Faghri [17], but was not used for this study. A second generation GDE was acquired from E-TEK, which had catalyst loadings of 4 mg cm^{-2} of Pt:Ru on the anode GDE and 4 mg cm^{-2} of Pt Black on the cathode GDE. A third generation GDE was also used from E-TEK which had loadings of 5 mg cm^{-2} Pt:Ru catalyst on the anode and 5 mg cm^{-2} Pt Black catalyst on the cathode. These layers have a porosity of about 70% and permeability of 4×10^{-10} m^{-2}. The manufacturer claims that the third generation GDEs has an improved anode structure for liquid feed of methanol and improved air cathode that is expected to experience some methanol crossover. Both second and third generation GDEs will be tested and compared for their effects on performance and water management.

The water management system developed in this study consisted of additional gas diffusion layers on the cathode side of the cell. The additional GDLs are thicker than normal, 480 μm compared to 350 μm, and have a higher loading of 50 wt% PTFE applied to them, which were custom designed and provided by E-TEK. The additional gas diffusion layer is placed between the cathode gas diffusion layer and cathode current collector. This increases the diffusion length and the hydraulic pressure on the cathode side of the cell. The net effect is that water is pushed back across the membrane due to the pressure gradient at the cathode. Four cell configurations were tested: configuration A with a Nafion® 117 membrane and no additional GDL, configuration B with a Nafion® 117 membrane and one additional GDL, configuration C with a Nafion® 117 membrane and two additional GDLs and configuration D which uses Nafion® 112 in the MEA and two additional cathode GDLs, shown in Fig. 3. Two different materials may be used for the water management layers in configurations C and D, however in this study, configurations with two additional cathode GDLs use the same material for each additional layer. Cells which use a second generation GDE are denoted by the subscript 2. For example a cell that had no additional cathode GDLs and used second generation anode and cathode GDEs is cell A_2. Cells that use a third generation GDE are denoted by the subscript 3. For example a cell that had no additional cathode GDLs and used third generation anode and cathode GDEs is cell A_3.

Once the cells are built, they are first tested to make sure there are no leaks. Then the membrane is hydrated and short-term performance evaluations, such as polarization curves are conducted on the cells to ensure proper function. If the performance is satisfactory then the long-term water management experiments are then conducted. The three steps needed to determine the water management characteristics of the cells are:

Step 1: diffusion, hydraulic permeation and evaporation testing.
Step 2: methanol crossover.
Step 3: constant current testing (long-term testing).

For step 1, the net transport of water by diffusion and hydraulic permeation was determined experimentally. The reservoir was filled with 10 g of DI water and sealed inside a container. This resembles a saturated environment, relative humidity of 100%, so that there is no water loss due to evaporation. Any remaining water in the reservoir after a long period of time, 1–2 days, allows for determination of water diffusion and permeation rate in the cell. Since the cell is air breathing the test was performed again in ambient conditions so that evaporation effects may be accounted for; relative humidity less than 100%. The loss of water will increase due to the driving force of evaporation at the cathode.

In step 2, the methanol crossover in the cells was determined for 1.0 mol kg^{-1}, 3.0 mol kg^{-1} and 5.0 mol kg^{-1} methanol solutions. The anode reservoir was filled with the solutions and run in open circuit voltage (OCV) mode. The initial solution weighed 10 g and the remaining solution after 6 h was measured. The amount of solution loss due to crossover was determined using the solution loss minus the evaporation of water, which can be determined from previous experiments.

In step 3, constant current experiments were run for three different solutions of 1.0 mol kg^{-1}, 3.0 mol kg^{-1} and 5.0 mol kg^{-1}. The cells were linked in series so that each cell could be run simultaneously. This allowed for each configuration to be run at the same current loading and environmental conditions, such that the only difference between cells was their structure. The cells were filled with 10 g of solution and the amount of solution remaining at the end of the test was weighed.

Table 1
Membrane electrode assembly, water management and air filter materials' properties

Material	Thickness (μm)	Mean pore diameter (μm)	Manufacturer
Nafion® 112	50.8		Dupont
Nafion® 117	180		Dupont
Anode/cathode GDE	350		E-TEK
Additional GDL	480	1.3	E-TEK
SPC Oil Sorbents	4770	18.8	Parmer Instrument Co.
Porous polyethylene I	2000	80–100	Small Parts Inc.
Porous polyethylene II	1000	10–20	Small Parts Inc.
ePTFE G110	250	0.5	Saint Gorbain

Once the water management system testing was completed the air management system was tested next. The four air filters tested were Oil Sorbents (OS), ePTFE, porous polyethylene I (PPI) and porous polyethylene II (PPII). The filters have different properties as listed in Table 1, such as thickness and mean pore size (MPS). The thickness of the filter plays a role in the trapping of particles as well as the amount of thermal insulation that the filter will provide. Each filter has a significant difference in thickness with Oil Sorbents being the thickest at 4.77 mm, porous polyethylenes I and II 2 mm and 1 mm, respectively, and ePTFE with a thickness of 250 μm. The MPS is important in determining the size of particle that can penetrate the filter. Oil Sorbents has a MPS of 18.8 μm, porous polyethylene I has a MPS of 80–100 μm, porous polyethylene II has a MPS of 10–20 μm and ePTFE has a MPS of 0.5 μm. The porosity of the filter plays an important role in the flow of air as well as blocking particles from entering the cathode of the cell. Oil Sorbents has porosity around 90% porous polyethylenes I and II have porosities of 80% and 50%, respectively and ePTFE has a porosity of 40%. The air filter was fit to the cathode opening and the edges were wrapped in Teflon tape to seal the filter to the frame. The configuration is shown in Fig. 2 and is referred to as E, which is nothing more than configuration C with the addition of an air filter.

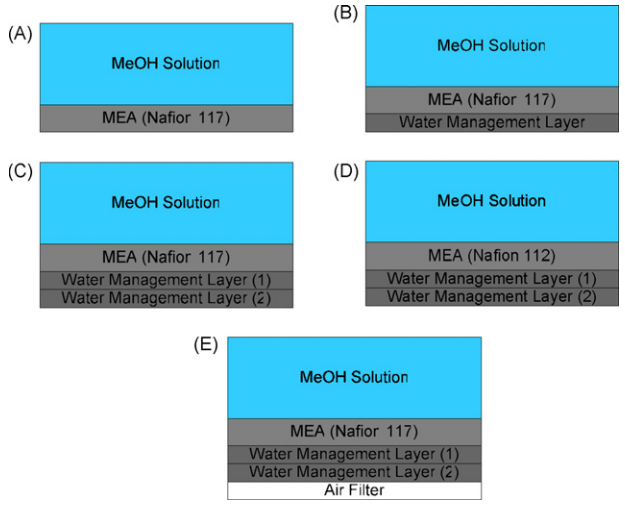

Fig. 2. Configurations A, B, C and D for water management and the air management configuration E.

A schematic and picture of the test setup is shown in Fig. 3. An integrated fuel cell test stand, Scribner 850C, was used to apply the load and record the current and power of the cells in series. The resistance of the cells was also measured to determine membrane hydration and was performed by an Agilent 4338B. An Agilent 34970 data acquisition unit, capable of recording 20 channels simultaneously, measured the thermocouples and voltage for each cell as well as ambient temperature. K-type thermocouples were placed next to the cathode gas diffusion layer to measure the temperature of the cell and they were also used to measure the ambient temperature. The Agilent equipment's data was recorded using Agilent's benchlogger software at 60 s intervals. Each cell was removed from the load when its voltage potential dropped below 0.1 V.

3. Results and discussion

The water management experiments were completed first, following the steps outlined in Section 2. The cells were tested simultaneously for each step to keep testing conditions the same for each cell. The air management experiments were completed next using two additional GDLs for the water management system. Each filter completed all the constant current experiments before switching to another filter. The four major parameters that were examined were the water balance coefficient, W_{BC}, power density, fuel utilization efficiency, η_{fuel}, and energy efficiency, η_{energy}.

Water flux through the membrane occurs via three processes, diffusion, hydraulic permeation and electro-osmotic drag. The sum of these three processes gives the total water flux as

$$j_{H_2O} = D\frac{\Delta c_{a\to c}}{L} + \frac{K}{\mu_{H_2O}}\Delta p_{a\to c}\frac{\rho_{H_2O}}{M_{H_2O}} + n_{EOD}\frac{I}{F} \quad (4)$$

where D is the diffusion coefficient, $\Delta c_{a\to c}$ the water concentration difference from anode to cathode, L the thickness of the membrane, K the permeability, μ_{H_2O} the viscosity of water, $\Delta p_{a\to c}$ the pressure difference from anode to cathode, ρ_{H_2O} the density of water, M_{H_2O} the molecular weight of water, n_{EOD} the electro-osmotic drag coefficient, I the current density and F is the Faraday constant [14]. These three terms are lumped together as the net water production in the cell.

To relate the amount of water used to methanol consumed, a water balance coefficient is defined as

$$W_{BC} = 2 - \frac{\text{water used (mol)}}{\text{methanol used (mol)}} \quad (5)$$

Based on our measurements, we calculate W_{BC} by

$$W_{BC} = 2 - \frac{[m_{Total} - m_{MeOH}]/M_{H_2O}}{m_i C_i - m_f C_f} \quad (6)$$

where m_{Total} is the total mass of solution used, m_{MeOH} the mass of methanol used, m_i the initial mass of solution, C_i the initial methanol concentration in mol kg^{-1}, m_f the final mass of solution and C_f is the final methanol concentration in mol kg^{-1}. This equation relates the amount of water used per methanol used in

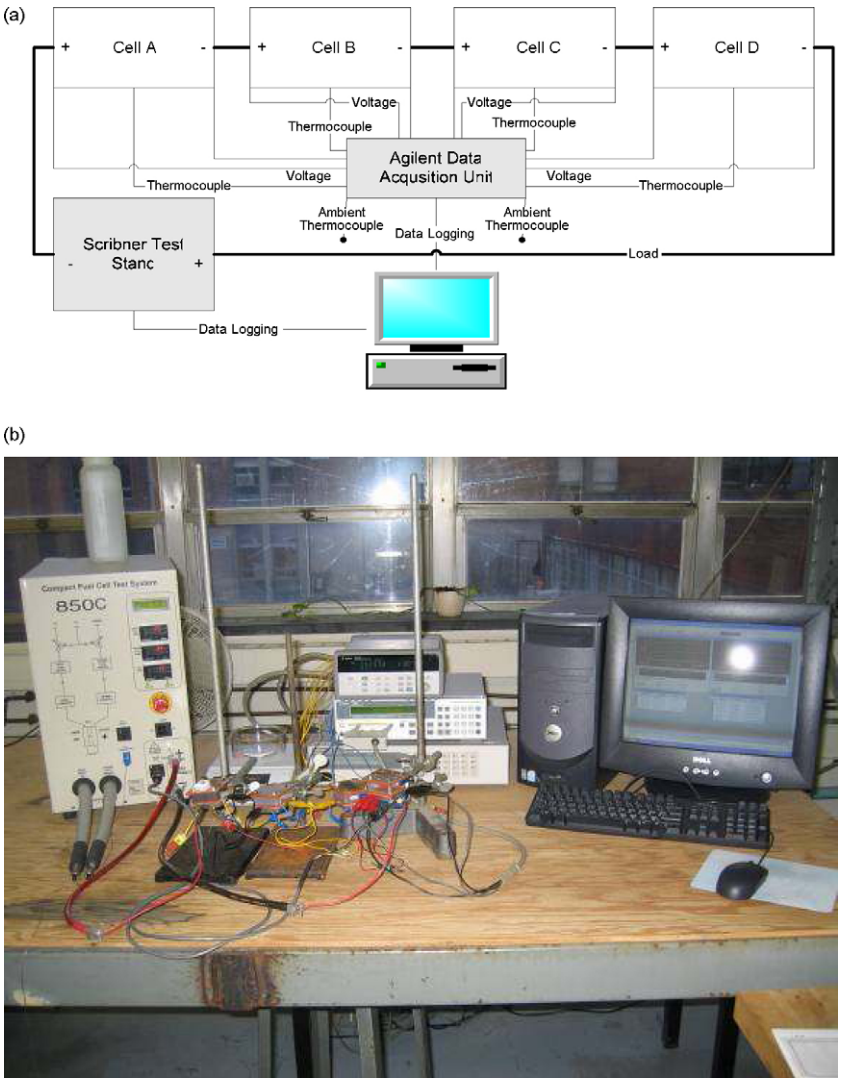

Fig. 3. (a) Schematic of test setup and (b) picture of test setup.

mole quantities. The overall reaction for a direct methanol fuel cell, Eq. (3), gives a net value of two molecules of water created during the reaction. When the W_{BC} is equal to zero, the system is losing 2 mol of water for every 1 mol of methanol consumed (the net product of 2 mol created by the reaction), which is water neutral operation. This is the ideal state for the cell to operate in, as suggested by Eq. (3). When the water balance coefficient is negative, there is an excess amount of water being lost or consumed; more than 2 mol of water used per mole of methanol used. When the water balance coefficient is positive, there is an excess amount of water being retained by the system; less than 2 mol of water used per mole of methanol used. This is the goal at which an external supply of water is not required.

To determine the concentration of methanol at the end of a test as in Eq. (6), dilute solutions were used to find the relative concentration at which the cells could no longer support the current loading. If the cell voltage showed a short stable region followed by a rapidly decreasing voltage over a 5 min period then it was estimated that this was the methanol concentration at the end of the specific test. This was compared to the experiments and used as the estimated final value of the methanol concentration. Using this information the total methanol consumed during the test can be found. The results for second generation cells, third generation cells and configuration D_3 are listed in Table 2 and the voltage versus time for a constant current are shown in Jewett [18].

The fuel utilization efficiency of the cells can be determined by comparing the methanol consumed by the reaction by the total methanol usage. The methanol consumption rate is calculated

Table 2
Final concentration of methanol at 0.1 V

Current (A)	Concentration (mol kg^{-1})		
	A_2, B_2, C_2	A_3, B_3, C_3	D_3
0.2	0.25	0.125	0.5
0.3	0.375	0.25	0.75
0.4	0.5	0.5	1.0
0.5		0.75	
0.6		0.85	

Table 3
Water management characteristics, resistance, diffusion and evaporation rates of each fuel cell

DMFC	Membrane	Additional GDLs	Resistance (mΩ)[a]	Diffusion ($g\,h^{-1}$)	Evaporation ($g\,h^{-1}$)[a]
A_2	Nafion® 117	0	63.5	0.018	0.096
B_2	Nafion® 117	1	76.8	0.023	0.085
C_2	Nafion® 117	2	64.5	0.016	0.076
A_3	Nafion® 117	0	72.2	0.020	0.201
B_3	Nafion® 117	1	58.5	0.013	0.109
C_3	Nafion® 117	2	62.6	0.007	0.096
D_3	Nafion® 112	2	35.1	0.012	0.112

[a] Temperatures of 20–30 °C and relative humidity of 10–36%.

as

$$j_{\mathrm{MeOH}} = \frac{IM_{\mathrm{MeOH}}}{6F} \tag{7}$$

where j is in $g\,s^{-1}$, I the current, M_{MeOH} the molecular weight of methanol and F is the Faraday constant. To find the total methanol consumed by the reaction, the methanol consumption rate is integrated over the time the cell operated. The total methanol used can be found by subtracting the initial concentration by the end concentration. The difference between the total methanol consumed and estimated concentration change gives the amount of methanol lost due to methanol crossover. The fuel utilization efficiency is defined as [19]:

$$\eta_{\mathrm{fuel}} = \frac{\int j_{\mathrm{MeOH}}\,\mathrm{d}t}{(m_{\mathrm{i}}C_{\mathrm{i}} - m_{\mathrm{f}}C_{\mathrm{f}})M_{\mathrm{MeOH}}} \tag{8}$$

The energy efficiency can also be found by taking into account the voltage and current of the cell [20]. We define the energy efficiency as

$$\eta_{\mathrm{energy}} = \frac{\int IV(t)\,\mathrm{d}t}{(m_{\mathrm{i}}C_{\mathrm{i}} - m_{\mathrm{f}}C_{\mathrm{f}})\mathrm{LHV}} \tag{9}$$

where $V(t)$ is the voltage and LHV is the lower heating value of methanol, $\mathrm{LHV}_{\mathrm{MeOH}} = 638.1\,\mathrm{kJ\,mol^{-1}}$.

3.1. Water management (second generation GDE)

Three cells were created with different water management configurations, A_2, B_2 and C_2 and their polarization curves were found to ensure that the cells were operating properly. The cells were tested using $3.0\,\mathrm{mol\,kg^{-1}}$ solution at ambient conditions ranging from 22 °C to 26 °C and relative humidity of 10–32%. The results of these tests can be seen in Fig. 4. All three of the cells share similar polarization curves with B_2 having a maximum power density of $20\,\mathrm{mW\,cm^{-2}}$ at $85\,\mathrm{mA\,cm^{-2}}$, C_2 having the next highest power density of about $16\,\mathrm{mW\,cm^{-2}}$ around $80\,\mathrm{mA\,cm^{-2}}$ and A_2 having a maximum power density of about $15\,\mathrm{mW\,cm^{-2}}$ at $60\,\mathrm{mA\,cm^{-2}}$.

3.1.1. Step 1: diffusion, hydraulic permeation and evaporation

To determine the diffusion and hydraulic permeation through each cell they were filled with 10 g of DI water and sealed inside a beaker. The conditions inside the beaker are assumed to be saturated so the only loss of water from the cell is through diffusion and hydraulic permeation. It was found that after 22.25 h cells A_2 and B_2 lost 0.392 g and 0.5052 g of water, respectively. Cell C_2 lost 0.324 g of water after 20 h in the sealed beaker. The rate of water loss from these cells is $0.0176\,\mathrm{g\,h^{-1}}$, $0.0227\,\mathrm{g\,h^{-1}}$ and $0.0162\,\mathrm{g\,h^{-1}}$ for cells A_2, B_2 and C_2, respectively.

To view the effects that evaporation plays on increasing water loss the cells were again filled with 10 g of DI water but left in ambient room conditions which were a temperature of 22 °C and relative humidity of 43%. After 24 h, cells A_2, B_2 and C_2 lost 2.3097 g, 2.0308 g and 1.8352 g, respectively. These are rates of about $0.096\,\mathrm{g\,h^{-1}}$, $0.085\,\mathrm{g\,h^{-1}}$ and $0.076\,\mathrm{g\,h^{-1}}$ for cells A_2, B_2 and C_2, respectively. The water management characteristics of each cell and their appropriate diffusion and evaporation rates are shown in Table 3.

Comparing the diffusion and evaporation losses of the three cells, it is clear that the addition of the water management layers decreased the rate of water loss especially due to evaporation. Cell B_2 had a water loss rate of $0.011\,\mathrm{g\,h^{-1}}$ less than cell A_2 and cell C_2 had a water loss rate of $0.009\,\mathrm{g\,h^{-1}}$ less than cell B_2. Also, the impact of evaporation on water loss from the cell is very significant with water loss rates tripling and quadrupling from diffusion to evaporation.

3.1.2. Step 2: methanol crossover

The cells were run in OCV mode using $1.0\,\mathrm{mol\,kg^{-1}}$, $3.0\,\mathrm{mol\,kg^{-1}}$ and $5.0\,\mathrm{mol\,kg^{-1}}$ solutions. Ambient conditions during testing ranged from 20 °C to 26 °C and 24% to 32% relative humidity. When using $1.0\,\mathrm{mol\,kg^{-1}}$ solution the rate of solution used in cells A_2, B_2 and C_2 were $0.093\,\mathrm{g\,h^{-1}}$, $0.087\,\mathrm{g\,h^{-1}}$ and $0.077\,\mathrm{g\,h^{-1}}$, respectively, as shown in Fig. 5. These values are very similar to the evaporation rates meaning that the addition of a small amount of methanol has very

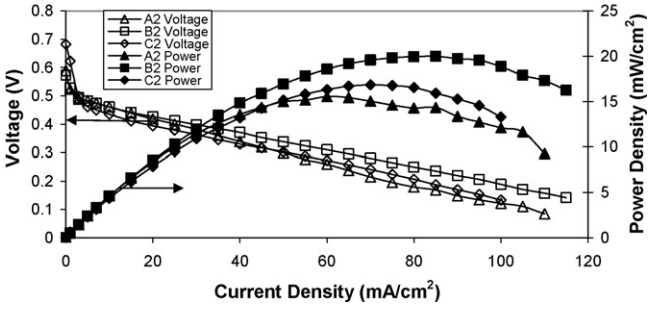

Fig. 4. Polarization curves for cells second generation cells using $3.0\,\mathrm{mol\,kg^{-1}}$ solution in ambient conditions of 23–26 °C and relative humidity of 10–32%.

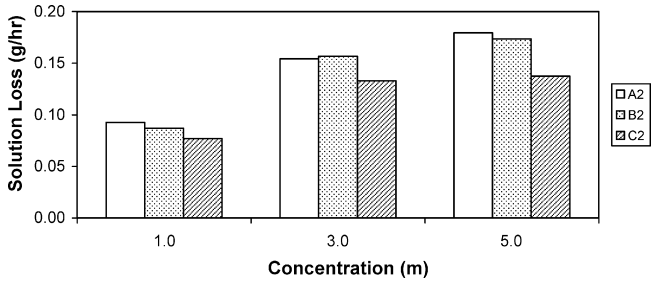

Fig. 5. Solution used per hour for second generation cells in ambient conditions of 20–26 °C and relative humidity of 24–32%, using 1.0 mol kg^{-1}, 3.0 mol kg^{-1} and 5.0 mol kg^{-1} for OCV conditions.

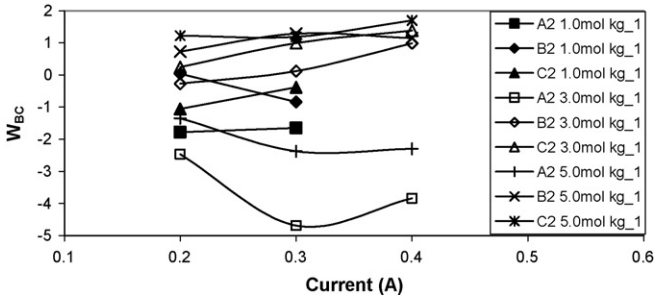

Fig. 6. Water balance coefficient for second generation cells under 0.2 A, 0.3 A and 0.4 A loadings using 1.0 mol kg^{-1}, 3.0 mol kg^{-1} and 5.0 mol kg^{-1} solutions in ambient conditions of 18–26 °C and relative humidity of 20–45%.

little effect on the loss of solution. When using 3.0 mol kg^{-1} solution the rates increased to 0.154 g h^{-1}, 0.157 g h^{-1} and 0.133 g h^{-1} and with 5.0 mol kg^{-1} the rates increased even more to 0.179 g h^{-1}, 0.174 g h^{-1} and 0.137 g h^{-1}, as shown in Fig. 5.

For each cell, as the concentration was increased from 1.0 mol kg^{-1} to 3.0 mol kg^{-1} and 3.0 mol kg^{-1} to 5.0 mol kg^{-1}, the rate of solution loss increased. This trend is caused by methanol crossover which increases as the concentration of methanol increases. Methanol crossover also increases the rate of evaporation of water from the fuel cell due to the increase in temperature that it causes. Also, the rates of solution loss between the cells have a similar trend as diffusion and evaporation. Cell C_2 had the lowest rate of solution loss while cell A_2 had the highest rate of solution loss. This again demonstrates the beneficial effects of the water management layers in slowing solution loss.

3.1.3. Step 3: constant current testing

When currents of 0.2 A, 0.3 A and 0.4 A were applied to the fuel cells the solution used during the tests increased even further. This is due to the increase in the electrochemical reaction to sustain the higher currents. Higher currents consume more solution because methanol is needed to support the loading and water is used in the reaction at a ratio of 1:1 as well as being pulled through the membrane by electro-osmotic drag. The solution used, time and charge from the constant current tests can be found in Jewett [11].

The water balance coefficients for each case were calculated using Eq. (6). For the 1.0 mol kg^{-1} cases it is observed that the cells have negative water balance coefficients for the 0.2 A and 0.3 A cases, as shown in Fig. 6. However, cells B_2 and C_2 are greater than −1 for each case while cell A_2 is less than −1.5 for both cases. This shows some improvement in the water balance coefficient with the addition of the water management layers. For 3.0 mol kg^{-1} solution cases cell A_2 continued to have a poor water balance coefficient, with values ranging between −2.463 and −4.685, as shown in Fig. 6. Cells B_2 and C_2 show significant improvement in the water balance coefficient with values ranging from −0.273 to 0.987 and 0.247 to 1.388, respectively. Cell C_2 satisfies the criteria for a water neutral operation for each loading. When using 5.0 mol kg^{-1} solution, it is again observed in Fig. 6, that cell A_2 has poor water balance coefficients ranging between −1.343 to −2.377. Cells B_2 and C_2 both have positive water balance coefficients with cell C_2 achieving a maximum of 1.697 for 0.4 A loading. These calculations show that the addition of the water management layers can significantly improve the water balance coefficient of a cell and achieve water neutral operation.

It is again found that the cells with water management layers have greater water balance coefficients than the cell without. This is expected as it was the goal of this study to achieve water neutral conditions or better, which cell C_2 satisfies for all the 3.0 mol kg^{-1} and 5.0 mol kg^{-1} cases. Cell B_2 also achieves water neutral conditions for some cases, but does not reach as high of water balance coefficient as cell C_2. The greatest increase in the water balance coefficient comes from the addition of one water management layer. The addition of a single water management layer increases the water balance coefficient by about 2 on average. The addition of a second water management layer has a lesser effect on the water balance coefficient and only increases it slightly. It was also noticed that as the concentration increased, the water balance coefficient also increased. This is due to more methanol being consumed and crossing over which allows for more water recovery and also increases the value of the water balance coefficient as defined in Eq. (6).

The fuel utilization efficiency, defined in Eq. (8), was calculated for each case. It is expected that the 5.0 mol kg^{-1} solution and low current cases will have poor efficiency due to methanol crossover. For 1.0 mol kg^{-1} solutions the efficiency decreases as the loading increases, with the cells having about 48% efficiency for 0.2 A case and 27% for the 0.3 A case, as shown in Fig. 7. This was caused by instability associated with low concentration solu-

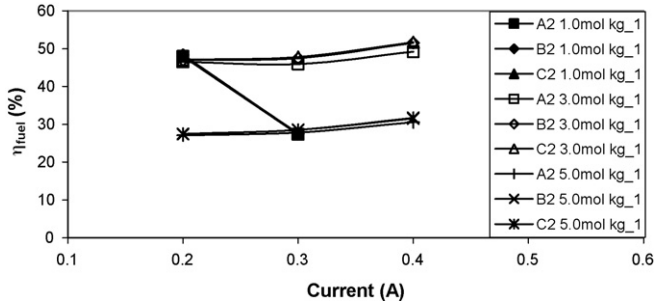

Fig. 7. Fuel utilization efficiency for second generation cells under 0.2 A, 0.3 A and 0.4 A loadings using 1.0 mol kg^{-1}, 3.0 mol kg^{-1} and 5.0 mol kg^{-1} solutions in ambient conditions of 18–26 °C and relative humidity of 20–45%.

tions which reduced the runtime of the cell and results in lower fuel utilization efficiency. The cells with 1.0 mol kg^{-1} solution could not support a loading of 0.4 A. For the 3.0 mol kg^{-1} cases the fuel efficiency of the cells was about the same, 46%, for 0.2 A loading, as shown in Fig. 7. As the loading was increased however, the fuel efficiency also increased to about 47% under 0.3 A and the maximum fuel efficiency of 51.7% was achieved under a 0.4 A loading for cell C_2. When 5.0 mol kg^{-1} solution was used the fuel efficiency decreased as expected due to methanol crossover, as shown in Fig. 7. The cells had an efficiency of about 27% for the 0.2 A case, which increased slightly to 28% and 31% for 0.3 A and 0.4 A cases, respectively. This reinforces the claim made earlier in the paper that the ideal concentration is about 3.0 mol kg^{-1} for passive DMFCs.

The fuel utilization efficiency was about the same for each cell for a given case. This is expected because there was no change to how the cell reaction proceeds. There was some slight increase in efficiency for cells B_2 and C_2 compared to A_2, however this was generally less than 1–2%. The important information obtained from the fuel efficiency was that the 3.0 mol kg^{-1} solution cases tend to have the greatest efficiency. This is expected because, as mentioned in Section 1, the ideal concentration at the anode is 2.0–3.0 mol kg^{-1} to reduce the amount of methanol crossover while not encountering a methanol mess transport limitation.

3.2. Water management (third generation GDE)

The polarization curves for cells A_3, B_3, C_3 and D_3 were found to ensure proper operation. The results for a 3.0 mol kg^{-1} solution are shown in Fig. 8. The range of current density that these cells can support is similar to the second generation cells however, the maximum power densities are greater. This is due to the improved anode and cathode GDEs. The second generation cells had maximum power densities in the range of 15–20 mW cm^{-2} while the third generation cells have maximum power densities in the range of 20–25 mW cm^{-2}.

3.2.1. Step 1: diffusion, hydraulic permeation and evaporation

The results of these tests are displayed in Table 3. Sealing the cells inside a container shows how the additional GDLs limit the amount of water diffusion and hydraulic permeation through the cell. Cell A_3 has a net rate of water loss of about 0.02 g h^{-1} while the addition of one GDL decreased the rate by 35% to 0.013 g h^{-1}. The addition of a second GDL decreased the rate of water loss by a further 30% to 0.007 g h^{-1}. Cell D_3 also showed some limiting of water loss however, due to the thinner membrane water has a shorter diffusion length and permeates through the cell easier. This means that despite having two additional GDLs the water loss from the cell is only decreased about 40% to a rate of 0.012 g h^{-1}.

The same experiment was run again only this time the cells were open to the ambient environment. The room conditions during the test averaged a temperature of about 25 °C with a relative humidity of 20%. The results show a similar trend as the diffusion and hydraulic permeation test. Cell A_3 has the highest rate of water loss of 0.201 g h^{-1} and cell B_3 shows a significant decrease in water loss with the addition of one GDL to 0.109 g h^{-1}, about 45%. Cell C_3 with two additional GDLs has very little improvement in water loss, 0.096 g h^{-1} about 10% less than cell B_3. This is a big difference when compared to the previous testing where cell C_3 further decreased the water loss by 30%. Cell D_3 had a loss of 0.112 g h^{-1} which is almost the same rate of water loss as cell B_3 which is similar to the diffusion and hydraulic permeation results.

Comparing the water loss rates of the evaporation and diffusion testing it is again found that the influence of evaporation significantly increases the rate of water loss. For these cells the evaporation rate increased the water loss by up to 10 times the diffusion rate. Cell A_3, which had no water management layer had the most significant effects by increasing from a diffusion water loss rate of 0.02 g h^{-1} to an evaporation rate of 0.20 g h^{-1}. Cells with water management layers also had significant evaporation effects with rates of about 0.1 g h^{-1}. This again shows the benefits of the water management layers in reducing the water loss from the cell.

3.2.2. Step 2: methanol crossover

OCV tests were conducted for all four cells using concentrations of 1.0 mol kg^{-1}, 3.0 mol kg^{-1} and 5.0 mol kg^{-1} to test the effects of methanol crossover. The solution used per hour is shown in Fig. 9. Again, similar trends as in the diffusion and evaporation experiments are found for these tests. Cell A_3 lost the most solution, 1.654 g, 2.304 g and 2.872 g for 1.0 mol kg^{-1}, 3.0 mol kg^{-1} and 5.0 mol kg^{-1} concentrations, respectively, while cells B_3 lost 1.064 g, 1.448 g and 2.060 g and C_3 lost 0.934 g, 1.438 g and 2.070 g. There is very little dif-

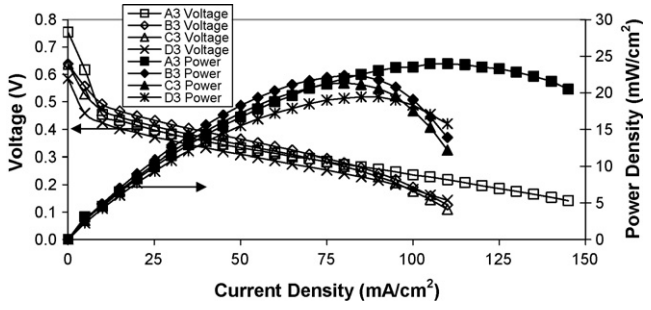

Fig. 8. Polarization curves of third generation cells using 3.0 mol kg^{-1} solution in ambient conditions of 19–26 °C and relative humidity of 20–50%.

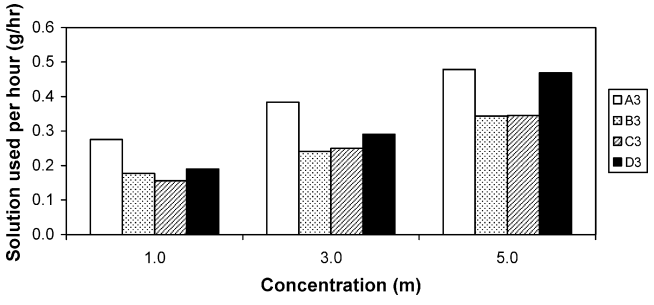

Fig. 9. Solution used per hour for third generation cells using 1.0 mol kg^{-1}, 3.0 mol kg^{-1} and 5.0 mol kg^{-1} for OCV conditions in ambient conditions of 25 °C and relative humidity of 10–20%.

ference in the amount of solution used between cells B_3 and C_3 and in some cases cell C_3 actually lost slightly more solution. Cell D_3 lost more solution, 1.140 g, 1.746 g and 2.812 g for 1.0 mol kg^{-1}, 3.0 mol kg^{-1} and 5.0 mol kg^{-1}, respectively, than cell B_3 for these cases due to increased methanol crossover. For the test using 5.0 mol kg^{-1} solution, cell D_3 lost almost the same solution as cell A_3. With a thinner membrane, methanol can crossover much easier and it was readily apparent based on the temperature of the cells that D_3 had more methanol crossover than the other three cells.

For these tests similar trends to second generation and previous testing are apparent. As the concentration increases, the amount of solution lost also increases due to the effects of methanol crossover. Also, cells with water management layers lose less solution than cells without water management layers. Cell D_3 is an exception to this due to its thinner membrane which allows for increased diffusion and methanol crossover, which both relate to more solution loss.

3.2.3. Step 3: constant current testing

For the 1.0 mol kg^{-1} cases, results were unstable due to the low concentration of the solution. Under a 0.2 A load the cells would run for about one hour, while for any higher loading the cells could not support voltages over 0.1 V for more than a few minutes.

For the 3.0 mol kg^{-1} cases, cells A_3 and D_3 were losing too much water for all cases, as shown in Fig. 10. Cell A_3 had water balance coefficients in the range of −0.287 for 0.5 A to −4.885 for 0.4 A. Cell D_3 also had poor water balance coefficients ranging from −1.420 for 0.2 A to −2.037 for 0.4 A. Cells B_3 and C_3's water balance coefficient were less than zero for the 0.2 A case. This could be due to the long period of time that the test is run for. Evaporation can play an important role during these longer tests and is most likely why the cells have a less than zero water balance coefficient. For the 0.3 A case, cells B_3 and C_3 had water balance coefficients just less than 1 which means that they were retaining about 1 mol of water per methanol mol consumed. For the 0.4 A case, cells B_3 and C_3's water balance coefficient were 0.662 and 0.578, respectively, which is greater than water neutral operation. The water balance coefficients decreased slightly for the 0.5 A case however they stayed above zero. Under a 0.6 A load cells B_3 and C_3 had water balance coefficients of 0.566 and 1.027, respectively. Cell D_3 could not support the higher loading and is thought to have gone through some degradation due to high temperatures caused by methanol crossover.

For the 5.0 mol kg^{-1} cases, it was found again that cells A_3 and D_3 both had negative water balance coefficients, meaning that too much water was being lost, as shown in Fig. 10. Cells B_3 and C_3, had water balance coefficients of −0.017 and 0.174, respectively, for the 0.2 A which is very close to water neutral conditions. For the other two loadings the water balance coefficients for cells B_3 and C_3 were between 0.5 and 1 for 0.3 A and greater than 1 for 0.4 A. Upon increasing the current loading to 0.5 A and 0.6 A it was observed that cell A_3 had an increase in the water balance coefficient. Cells B_3 and C_3 however decreased slightly from the 0.4 A water balance coefficient's value. The addition of the water management layers allows the cell to recover enough water so that external water does not need to be supplied. However, this only applies to cells using a thick, Nafion® 117, membrane as the thinner membrane, Nafion® 112, cannot operate at water neutral conditions.

For the third generation cells there is no clear trend as to how the water balance coefficient behaves as the concentration of the solution is increased. For the 0.3 A loading the water balance coefficient for cells B_3 and C_3 decreases as the solution is increased. However, for the 0.4 A loadings, the maximum water balance is achieved for 1.0 mol kg^{-1} and 5.0 mol kg^{-1} tests while the minimum is calculated for 3.0 mol kg^{-1} solution. The water balance coefficients for each cell still followed the expected trend however. Cell A_3 always had a lower coefficient than cell B_3, and cell C_3 generally had the highest water balance coefficient. Cell D_3 also had a low water balance coefficient, usually less than zero and for 1.0 mol kg^{-1} and 3.0 mol kg^{-1} cases it is higher than cell A_2, however for 5.0 mol kg^{-1} solutions it had the lowest water balance coefficient overall.

When calculating the fuel utilization efficiency it was found that for 1.0 mol kg^{-1} cases the results were unstable and did not make sense due to the instability of the cells. When 3.0 mol kg^{-1} solution was used the results were much more stable and followed the expected trend of increasing efficiency with loading. The efficiency increased from 37% to 61% as the loading increased from 0.2 to 0.6 for cells A_3, B_3 and C_3. Cell D_3 consistently had higher fuel utilization efficiencies as shown in Fig. 11. This is due to the higher concentration at the end of the tests that remains in the cell, which when inserted into Eq. (8) increases the efficiency of the cell. If the end concentration was the same

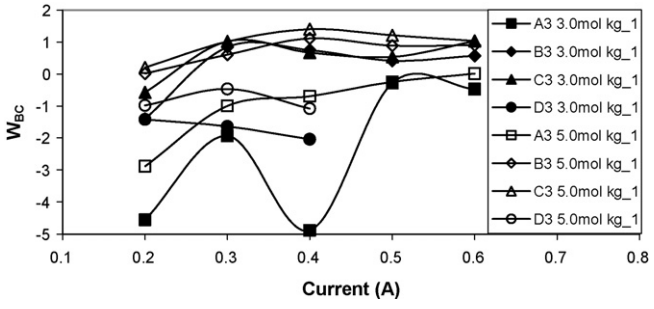

Fig. 10. Water balance coefficient for third generation cells under 0.2 A, 0.3 A and 0.4 A loadings using 3.0 mol kg^{-1} and 5.0 mol kg^{-1} solutions in ambient conditions of 18–26 °C and relative humidity of 15–50%.

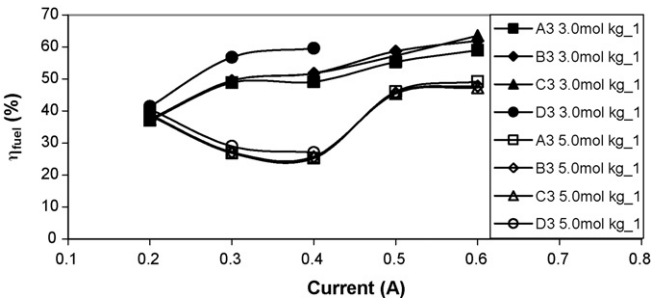

Fig. 11. Fuel utilization efficiency for third generation cells under 0.2 A, 0.3 A and 0.4 A loadings using 3.0 mol kg^{-1} and 5.0 mol kg^{-1} solutions in ambient conditions of 20–25 °C and relative humidity of 15–50%.

as the other three cells, the calculated efficiency would be about the same.

The 5.0 mol kg^{-1} solution tests had much lower fuel utilization efficiencies, less than 50% due to a significant amount of methanol crossover that occurs in high concentration solutions, Fig. 11. Also, it was found for the 3.0 mol kg^{-1} tests that as the loadings were increased the efficiency increased from 37% under 0.2 A loading to 50% under 0.3 A and 53% under 0.4 A. Again, this occurs because the reaction requires more methanol which reduces the amount that can crossover. For the 5.0 mol kg^{-1} cases it was observed that the fuel utilization efficiency decreased as the loading increased, until 0.5 A at which the fuel utilization efficiency jumps to about 45%. The fuel utilization efficiency continues to increase to 47–49% at 0.6 A. Under a 0.2 A load the cells had a fuel utilization efficiency of about 38% which decreased to 25% under a 0.4 A load. Again, this information supports the claim that a 3.0 mol kg^{-1} is the ideal concentration of methanol in a passive DMFC.

The energy efficiency of the cells was also calculated by Eq. (9) and the results are shown in Fig. 12. The maximum energy efficiency was found for 3.0 mol kg^{-1} solutions for each cell, ranging between 14% and 18% for cells A_3, B_3 and C_3. It is expected that the energy efficiency increase with loading however under loadings of 0.5 A and 0.6 A the efficiency decreased. This could be due to cell degradation as these tests were performed last and after many hours of operation for each cell. For 5.0 mol kg^{-1} solutions the efficiency is less than the 3.0 mol kg^{-1} cases and decreases with loading instead of increasing, for loadings less the 0.5 A. The lower efficiency compared to the 3.0 mol kg^{-1} cases is due to increased methanol crossover which wastes fuel by generating heat. Cells A_3, B_3 and C_3 are closely grouped together for both 3.0 mol kg^{-1} and 5.0 mol kg^{-1} solutions. Cell D_3 however is much lower than the other three cells for both solutions. The reason is similar for energy efficiency as it was for fuel utilization efficiency, which is increased methanol crossover due to the thinner membrane.

The efficiency of the cells with respect to concentration followed the expected trend. The 3.0 mol kg^{-1} cases had the highest efficiency with maximum fuel utilization efficiencies around 61% during 0.6 A testing. The 5.0 mol kg^{-1} cases had lower fuel utilization efficiencies due to methanol crossover effects with values ranging between 25% and 38%. An interesting phenomena to note for the 5.0 mol kg^{-1} cases is that the efficiency decreased as the loading increased, for loadings of 0.2–0.4 A, which is opposite from what is expected. Energy efficiencies are much lower than fuel utilization efficiencies with the maximum energy efficiencies ranging between 14% and 18%. This is caused by methanol crossover and the irreversibility of the reaction and the heat that is generated and wasted.

3.3. Air management (second generation GDE)

Using the two additional GDL configuration, C_2, from the water management experiments the air management system was tested next. The power density of C_2, from the water management tests, under a loading of 0.3 A and a concentration of 3.0 m was about 12 mW cm^{-2} with no filter. The addition of an air filter should ideally not decrease the average power density or the runtime of the cell. The cell was run using three methanol concentrations 1.0 mol kg^{-1}, 3.0 mol kg^{-1} and 5.0 mol kg^{-1}, with three loadings each of 0.2 A, 0.3 A and 0.4 A. The ambient conditions ranged from 20 °C to 30 °C and 20% to 70% relative humidity. The results for the 3.0 mol kg^{-1}, 0.3 A case for all air filters are shown in Fig. 13. The average power density for all cases was fairly similar and ranged between 11 mW cm^{-2} and 12 mW cm^{-2}. The major difference was the runtime of the cell with each filter. When the cell was run with no filter it ran for 9 h before dropping below the voltage limit, 0.1 V. When the cell had Oil Sorbents and ePTFE filters it lasted for 7.3 h and 8.0 h, respectively. However, the cases which used the porous polyethylene filters only lasted about 6.5 h.

3.3.1. Step 3: constant current testing

The results for 1.0 mol kg^{-1} solutions were unstable for the air management testing. Methanol mass transport limitations made for very unpredictable runtimes, water management and efficiencies.

For 3.0 mol kg^{-1} cases it was found that the air filters increased the water balance coefficient for all cases over cell C_2 initial performance without a filter, as shown in Fig. 14. The air filter with the highest water balance coefficient changed each test with PPI having a coefficient of 1.727 for 0.2 A loads, Oil Sorbents having a coefficient of 1.735 for 0.3 A loads and PPI having a coefficient of 2.055 for 0.4 A loads. An interesting thing to note is the shape of the water balance curves in Fig. 14. Oil Sorbents water coefficient takes on a concave shape with the

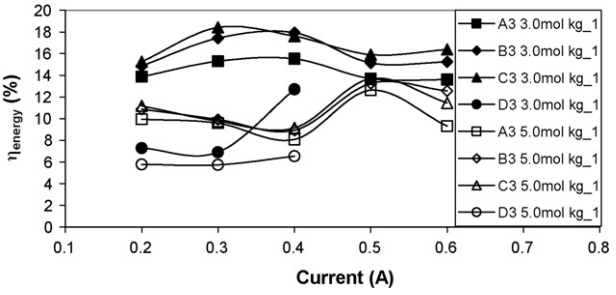

Fig. 12. Energy efficiency for third generation cells under 0.2 A, 0.3 A and 0.4 A loadings using 3.0 mol kg^{-1} and 5.0 mol kg^{-1} solutions in ambient conditions of 20–25 °C and relative humidity of 15–50%.

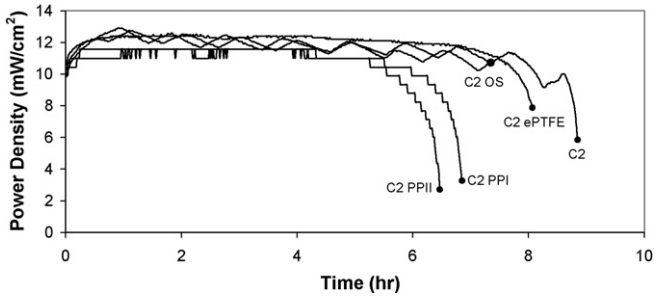

Fig. 13. Power density longevity of cell C_2 with four different air filters using 3.0 mol kg^{-1} solution under a 0.3 A load in ambient conditions of 20–30 °C and relative humidity of 20–80%.

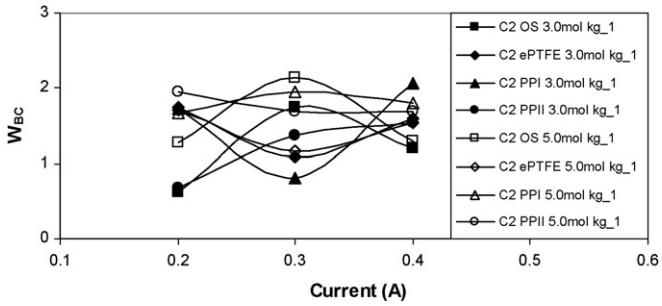

Fig. 14. Water balance coefficient for cell C_2 with air filters under 0.2 A, 0.3 A and 0.4 A loadings using 3.0 mol kg^{-1} and 5.0 mol kg^{-1} solutions in ambient conditions of 20–30 °C and relative humidity of 20–80%.

maximum occurring at 0.3 A. The cell without an air filter and PPII have a curve that increases with loading and ePTFE and PPI have convex curves with minimums occurring at 0.3 A.

The water balance coefficients for 5.0 mol kg^{-1} solutions were all greater than 1, as shown in Fig. 14. It was again found that the highest water balance coefficient occurred with different air filters for each loading. PPII had the highest water balance coefficient for 0.2 A of 1.952, Oil Sorbents had the highest coefficient for 0.3 A of 2.134 and PPI had the best coefficient for 0.4 A of 1.803.

It is difficult to make comparisons based on concentration and air filter for the water balance coefficient as it varied for each case and no clear trends were found. Each air filter did increase the water balance coefficient greater than the cell without an air filter though. This shows that the air filters can increase the water balance in the cell by limiting the evaporation of fluid from the cell.

The efficiency of the cell was increased for most of the filters when using 3.0 mol kg^{-1} solution, most notably for Oil Sorbents which achieved an efficiency of 64% for the 0.4 A case. The cell with a PPI filter was the only cell to have worse efficiencies for each case. The other filters showed a much more stable efficiency with smaller ranges, as shown in Fig. 15, for example ePTFE had efficiencies between 52% and 56% and PPII had efficiencies between 42% and 50%.

For the 5.0 mol kg^{-1} solutions, the Oil Sorbents filter increased the efficiency to 47% for the 0.4 A case. The best fuel utilization efficiency was 53% for the ePTFE filter under a 0.3 A

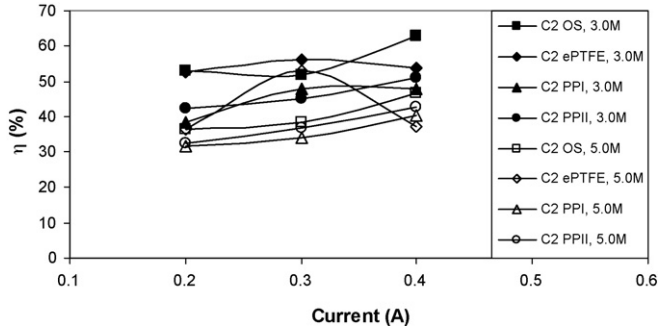

Fig. 15. Fuel utilization efficiency for cell C_2 with air filters under 0.2 A, 0.3 A and 0.4 A loadings using 3.0 mol kg^{-1} and 5.0 mol kg^{-1} solutions in ambient conditions of 20–30 °C and relative humidity of 20–80%.

loading. Examining Fig. 15, it is clear that each filter increased the efficiency of the cell with the efficiency increasing as the loading increased. The ePTFE filter is the only filter that did not follow this trend however and it has a concave shape with the maximum occurring at 0.3 A.

The addition of an air filter improved the efficiency for most cases. Maximum efficiencies were achieved using 3.0 mol kg^{-1} solutions and 5.0 mol kg^{-1} solutions having lower efficiencies as expected. The Oil Sorbents filter had the highest and most stable increase in efficiency compared to the other filters.

Based on the information collected for the different air filters, the Oil Sorbents filter was selected as the preferred filter for a number of reasons. It reduced the amount of solution used for almost every case, improved the water balance coefficient for almost every case and had the best and most stable efficiency improvement. Also due to its thick and porous structure, it will provide the most protection against airborne particles while still allowing sufficient air to pass through to the cathode.

3.4. Air management (third generation GDE)

Using the information from the previous air management testing, the air management experiments for third generation GDEs were completed for all four configurations using only the Oil Sorbents filter. Cell configurations will be distinguished using the water management configuration followed by the air filter abbreviation, i.e. OS.

3.4.1. Step 1: evaporation

Significant improvements in water retention and solution loss were achieved. The evaporation of water from the cell was reduced by over 50% with the addition of the air filter. The lowest evaporation rate without an air filter was 0.096 g h^{-1} for cell C_3 and even the highest evaporation rate for any of the cells with an air filter is 0.075 g h^{-1}. The evaporation rate of water from the cells decreases as the number of water management layers increases, down to a minimum of 0.062 g h^{-1} for cell C_3 OS. Cell D_3 OS, which uses Nafion® 112 for a membrane and has two additional cathode GDLs, had a higher evaporation rate than cell C_3 OS, which also has two additional GDLs. The thinner membrane allows for diffusion and hydraulic permeation to play a larger role in water transport which increases the rate of water loss from the cell.

3.4.2. Step 2: methanol crossover

OCV tests were conducted for all four cells using concentrations of 1.0 mol kg^{-1}, 3.0 mol kg^{-1} and 5.0 mol kg^{-1} to test the effects of methanol crossover. The solution used per hour is shown in Fig. 16. For 1.0 mol kg^{-1} the results are varied, with cell A_3 OS using the least amount of solution and cell B_3 using the most solution. The typical trend is cell A_3 using the most solution, followed by cell D_3. Cell D_3 OS used the same amount of solution as cell B_3 OS, 0.096 g, however this is expected due to the thinner membrane in cell D_3. For the 3.0 mol kg^{-1} case cell A_3 OS used the most solution of 0.950 g while cells B_3 OS and C_3 OS used decreasingly less, 0.824 g and 0.790 g, respectively, which follows the trend from previous tests. Cell D_3 OS

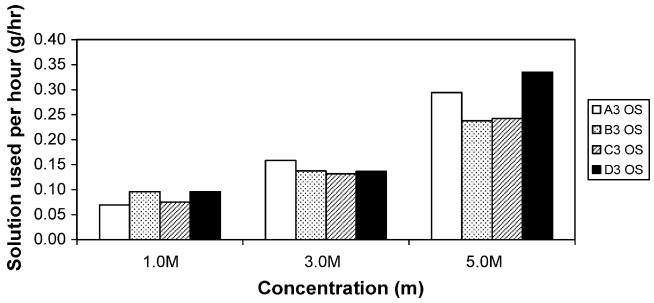

Fig. 16. Solution used per hour for third generation cells using 1.0 mol kg^{-1}, 3.0 mol kg^{-1} and 5.0 mol kg^{-1} at OCV conditions in ambient conditions of 25 °C and relative humidity of 20–36%.

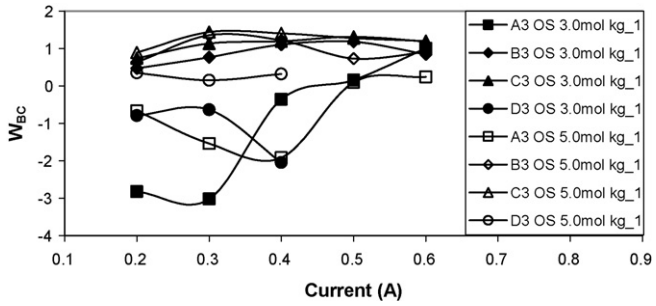

Fig. 17. Water balance coefficient for third generation cells with an Oil Sorbents air filter under 0.2 A, 0.3 A and 0.4 A loadings using 3.0 mol kg^{-1} and 5.0 mol kg^{-1} solutions in ambient conditions of 22–27 °C and relative humidity of 15–45%.

used slightly more solution than cell C_3 OS, 0.820 g, which is also expected. For the 5.0 mol kg^{-1} case cell D_3 OS used the most solution, 2.01 g, which topped cell A_3 which used 1.766 g. This is due to the increased methanol crossover that takes place in cell D_3 due to its thinner membrane. Cells B_3 OS and C_3 OS used 1.426 and 1.456, respectively.

When comparing the air management and water management results for OCV cases, it is clearly seen that the tests with an air filter used much less solution than the water management experiments. The reduced rate of evaporation caused by the air filter helps to limit the loss of solution from the cell. This is a trend that will continuously be seen in the air filter testing. Continuing the trends from the water management experiments, the cells lose more solution as the concentration increases due to methanol crossover, and cells which have water management layers, B_3 OS and C_3 OS, use less solution than cells that do not, A_3 OS. Cell D_3 OS continued to be the exception, as was the case for the water management tests, in that it used more solution than cell C_3 OS and used the most solution for the 5.0 mol kg^{-1} case.

3.4.3. Step 3: constant current testing

The 1.0 mol kg^{-1} test results were again very unstable due to the low concentration solution used for constant current testing. Methanol mass transport limitation occurred very quickly and resulted in very short tests. Uncharacteristic water balance coefficients and efficiencies were calculated due to the short testing times.

For 3.0 mol kg^{-1} solutions the water balance coefficients were negative for current between 0.2 A and 0.4 A for cells A_3 OS and D_3 OS, as shown in Fig. 17. For cells B_3 OS and C_3 OS the water balance coefficient was 0.443 and 0.721 for the 0.2 A case, 0.723 and 1.099 for the 0.3 A case and 1.036 and 1.129 for the 0.4 A case, respectively. At higher currents of 0.5 A and 0.6 A the water balance coefficient stayed consistent with little change in their values for cells B_3 and C_3. For 5.0 mol kg^{-1} solutions, cell B_3 OS had water balance coefficients that ranged between 0.6 and 1.3, and cell C_3 OS had water balance coefficients in the range of 0.8–1.4, as shown in Fig. 17. Cell A_3 OS had negative coefficients for each loading and cell D_3 OS had water balance coefficients that ranged between 0.15 and 0.35.

When the concentration is increased from 1.0 mol kg^{-1} to 3.0 mol kg^{-1} a decrease in the water balance coefficient is observed for all cases. This is due to the longer runtime that the cells experience with the higher concentration. This allows more time for methanol and water to crossover and evaporate which will reduce the water balance coefficient. When the concentration is increased from 3.0 mol kg^{-1} to 5.0 mol kg^{-1} the water balance coefficients increase due to more methanol being used or crossing over. By Eq. (6), the more methanol that is used the higher the water balance coefficient will become. Also, following the trend from the water management experiments, cells B_3 OS and C_3 OS, which have water management layers, have the best water balance coefficients and cell A_3 OS has the lowest water balance coefficient as expected.

When using 3.0 mol kg^{-1} solutions the fuel utilization efficiency increased from 41% to 60% as the loading was increased. Comparing these values to the water management cases it was observed that the 0.2 A loading's efficiency increased, however the cases from 0.3 A to 0.6 A decreased, Fig. 18. For 5.0 mol kg^{-1} cases the fuel utilization efficiency is lower than the 3.0 mol kg^{-1} cases, Fig. 18. This is due to the increase in methanol crossover which is the primary source of methanol fuel inefficiency. The fuel utilization efficiency increased as the loading increased from 31% at 0.2 A to about 45% at 0.6 A. The fuel utilization efficiency of cell D_3 OS was even lower with values between 16% and 19%.

The fuel utilization efficiency follows the same trend as the water management tests, where the best efficiency occurs using 3.0 mol kg^{-1}. The 5.0 mol kg^{-1} is much less efficient due

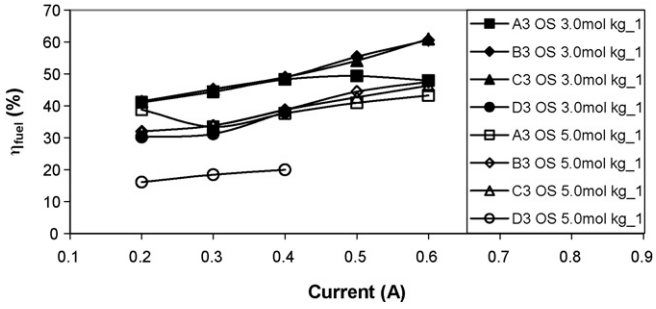

Fig. 18. Fuel utilization efficiency for third generation cells with an Oil Sorbents air filter under 0.2 A, 0.3 A and 0.4 A loadings using 3.0 mol kg^{-1} and 5.0 mol kg^{-1} solutions in ambient conditions of 22–27 °C and relative humidity of 15–45%.

to methanol crossover and the 1.0 mol kg^{-1} cannot function long enough to make it efficient. Comparing the water management cases to the air management cases, it was found that for 3.0 mol kg^{-1} solutions the air filter decreases the efficiency slightly, and for 5.0 mol kg^{-1} solutions the efficiencies calculated are about the same.

4. Conclusions

The goal of a water neutral or better operation was successfully achieved. The additional thick GDLs on the cathode side increased the hydraulic pressure which forced water back to the anode side of the cell. Water balance coefficients of 0.996 and 1.021 were achieved for 3.0 mol kg^{-1} solution under a 33 mA cm^{-2} load for second and third generation cells, respectively. The use of two additional GDLs is recommended even though the use of only one GDL may allow the cell to achieve water neutral conditions with a Nafion® 117 membrane. The additional GDL will reduce the amount of water lost to evaporation when it is not in operation.

The addition of the air filter reduced the evaporation of water from the cell which improved the water balance coefficient and provided thermal insulation. The difference between the filters was varied however the Oil Sorbents filter was chosen based on its good overall water management and efficiency as well the deep filtration characteristics of the material. There was some small efficiency loss with the air filter however the normal operational power density of the cell was unaffected. This loss of efficiency may have been caused by saturation of the filter especially at the end of tests. For the case of 3.0 mol kg^{-1} solution under a 33 mA cm^{-2} load using third generation GDEs, a 4.3% decrease in efficiency was observed. On the other hand, the water balance coefficient was increased from 1.021 to 1.131 for the same case and cell.

The thicker membrane, Nafion® 117, performed significantly better than the thinner membrane, Nafion® 112, for water management and efficiency. The thicker membrane reduces the amount of diffusion and EOD that takes place in the cell. For a loading of 33 mA cm^{-2} using 3.0 mol kg^{-1} solution the water balance coefficients for Nafion® 117 and Nafion® 112 were 1.021 and −1.637, respectively. The energy efficiency for the same case was 18.4% for Nafion® 117 compared to 6.9% for Nafion® 112. This reduction in efficiency was predominantly due to the increase in methanol crossover for Nafion® 112 cells. Another important fact to mention is the longevity of the cells with different membranes. Cells which used Nafion® 117 membranes showed very little degradation of power throughout testing. Cell D_3, which used Nafion® 112, showed a steady decrease in performance throughout testing and could not support high loadings, 0.5 A and 0.6 A, by the end of testing.

The third generation anode and cathode GDEs improved the maximum cell power density by up to 5 mW cm^{-2} for each configuration when using 3.0 mol kg^{-1} solution. The maximum power density using a 3.0 m solution under a loading of 33 mA cm^{-2} was increased from 20 mW cm^{-2}, for second generation cells, to 25 mW cm^{-2}, for third generation cells. The water balance coefficient and fuel utilization efficiency of the cells were mostly unaffected by the different GDEs.

References

[1] B. Bae, B.K. Kho, T.-H. Lim, I.-H. Oh, S.-A. Hong, H.Y. Ha, J. Power Sources 158 (2006) 1256–1261.
[2] D. Kim, E.A. Cho, S.-A. Hong, I.-H. Oh, H.Y. Ha, J. Power Sources 130 (2004) 172–177.
[3] Y.-J. Kim, B. Bae, M.A. Scibioh, E.A. Cho, H.Y. Ha, J. Power Sources 157 (2006) 253–259.
[4] T. Shimizu, T. Momma, M. Mohamedia, T. Osaka, S. Sarangapani, J. Power Sources 137 (2004) 277–283.
[5] Z. Guo, Y. Cao, J. Power Sources 132 (2004) 86–91.
[6] B.K. Kho, B. Bae, M.A. Scibioh, J. Lee, H.Y. Ha, J. Power Sources (2004).
[7] A. Faghri, Z. Guo, Int. J. Heat Mass Transfer 48 (2005) 3891–3920.
[8] F. Liu, G. Lu, C.-Y. Wang, J. Electrochem. Soc. 153 (2006) 543–553.
[9] X. Ren, W. Henderson, S. Gottesfeld, J. Electrochem. Soc. 144 (1997) 267–270.
[10] X. Ren, S. Gottesfeld, J. Electrochem. Soc. 148 (2001) 87–93.
[11] F.Y. Zhang, X.G. Yang, C.Y. Wang, J. Electrochem. Soc. 153 (2006) 225–232.
[12] E. Peled, A. Blum, A. Aharon, M. Philosoph, Y. Lavi, Electrochem. Solid-State Lett. 6 (2003) 268–271.
[13] A. Blum, T. Duvdevani, M. Philosoph, E. Rudoy, E. Peled, J. Power Sources 117 (2003) (2003) 22–25.
[14] G.Q. Lu, F.Q. Liu, C.-Y. Wang, Electrochem. Solid-State Lett. 8 (2005) 1–4.
[15] H. Kim, J. Oh, J. Kim, H. Chang, J. Power Sources 162 (2006) 497–501.
[16] Z. Guo, A. Faghri, J. Power Sources (2006) 1142–1155.
[17] Z. Guo, A. Faghri, J. Power Sources 160 (2006) 1183–1194.
[18] G. Jewett, Thesis, University of Connecticut, 2007.
[19] J.G. Liu, T.S. Zhao, Z.X. Liang, R. Chen, J. Power Sources (2005).
[20] J.G. Liu, T.S. Zhao, R. Chen, C.W. Wong, Electrochem. Commun. 7 (2005) 288–294.